National Aeronautics and Space Administration
Jet Propulsion Laboratory
California Institute of Technology

Insights into tropospheric chemistry: new results utilizing EOS TES, OMI, and MOPITT

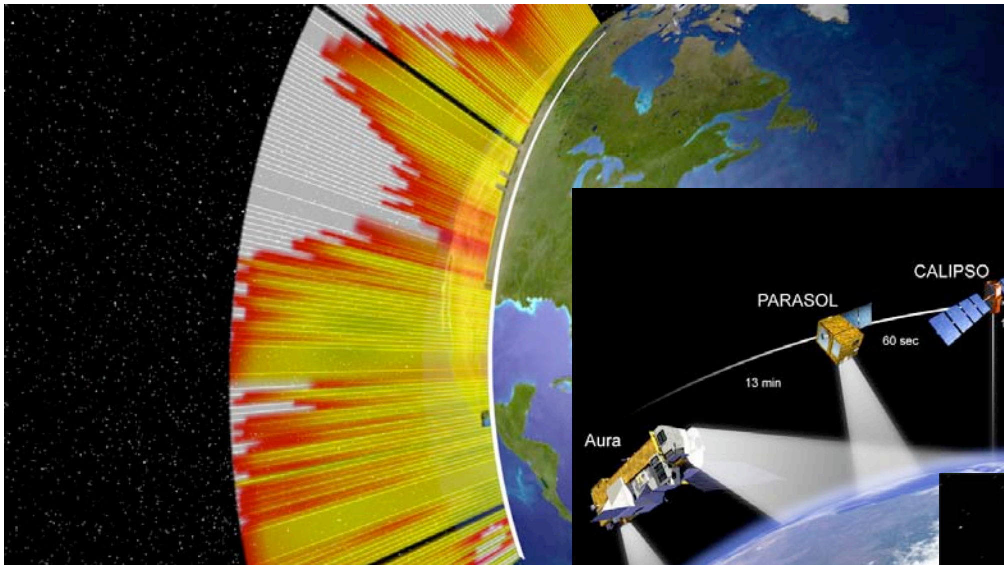

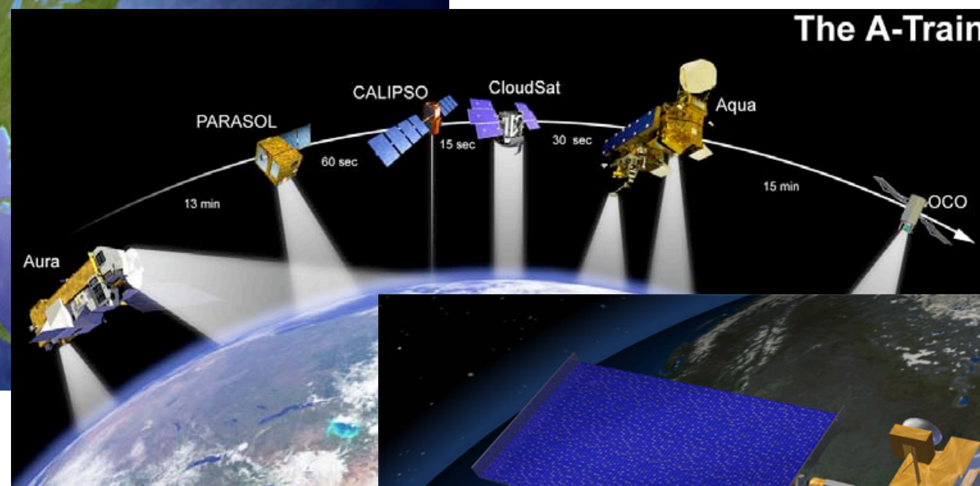

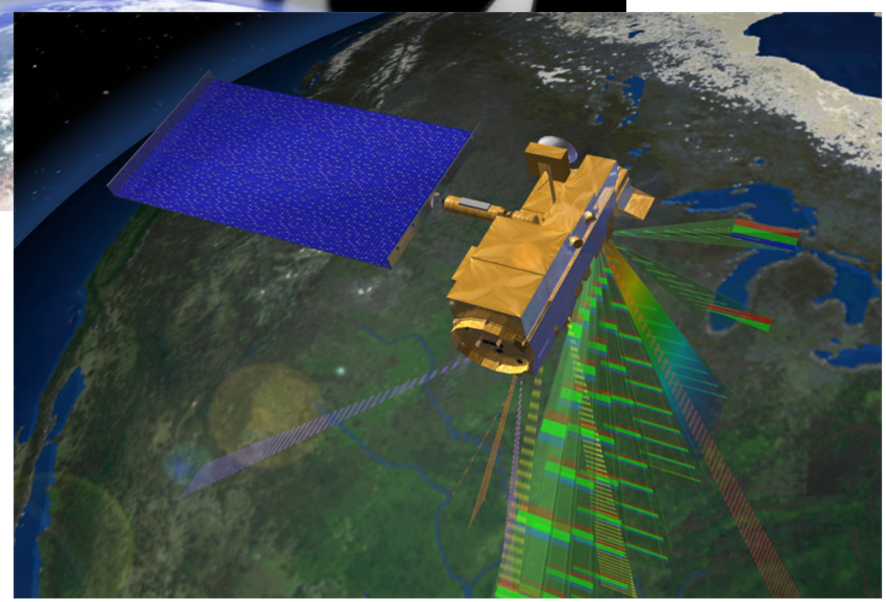

Annmarie Eldering[1] (presenting), K. Bowman[1], J. Worden[1], R. Beer[1], P.K. Bhartia[2], P. Levelt[3], J. Gille[4], D. Edwards[4], M. Detter[4]

National Aeronautics and Space Administration
Jet Propulsion Laboratory
California Institute of Technology

Tropospheric chemistry is a complex problem!

Anthropogenic sources

Natural precursors

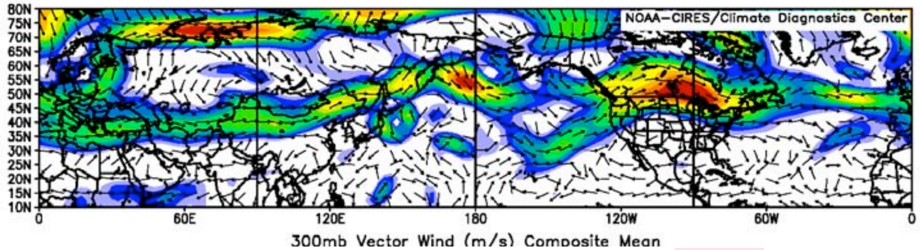

Advection

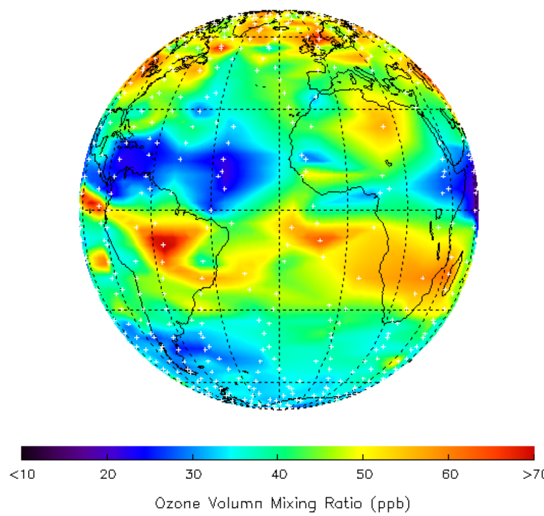

Global TES ozone

Solar radiation

Convection

Subsidence

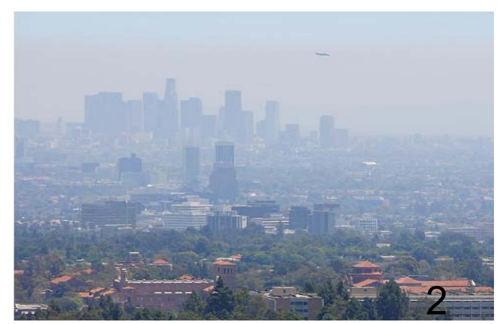

Tropospheric Emission Spectrometer

TES Movie

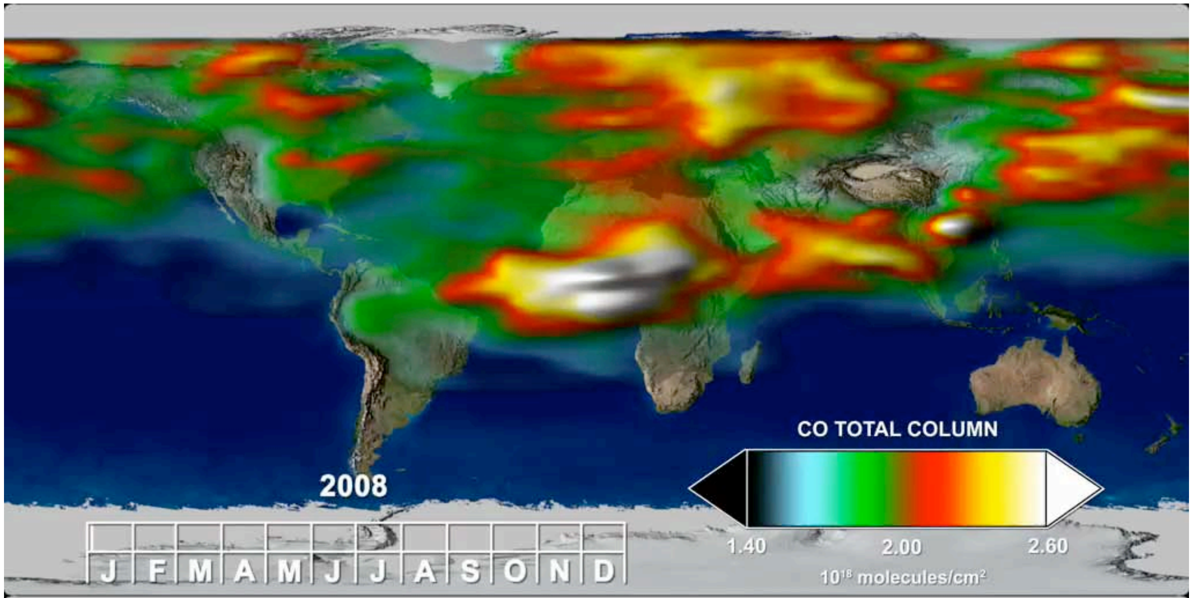

One year of TES CO

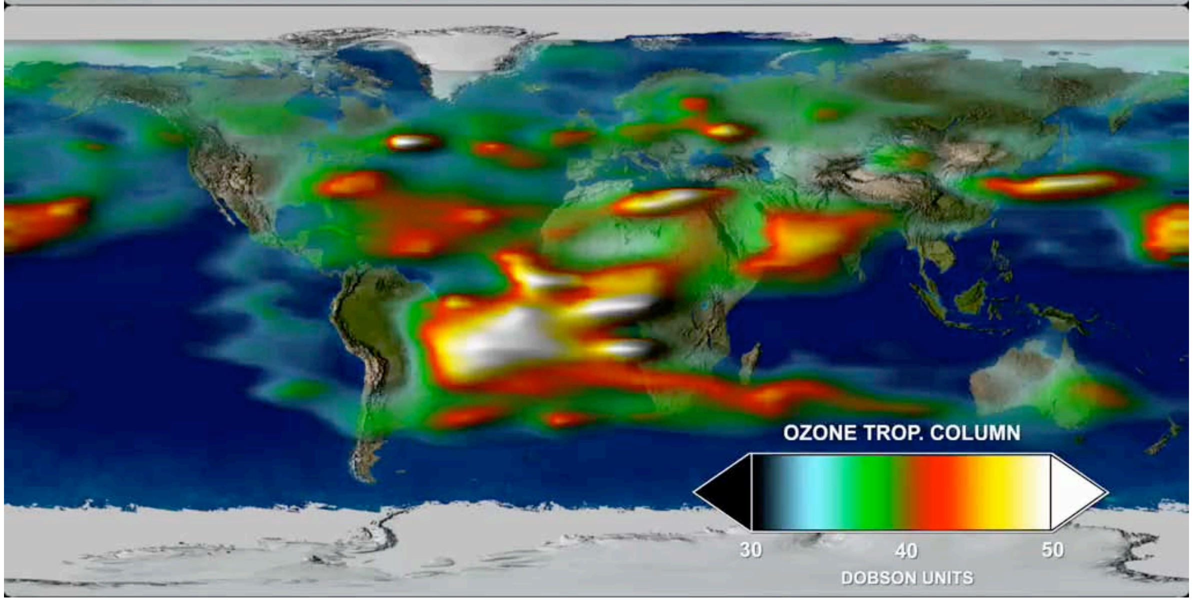

One year of TES O_3

National Aeronautics and Space Administration
Jet Propulsion Laboratory
California Institute of Technology

The tropical Atlantic ozone “paradox”

MODIS firecounts Jan 11-21, 2005

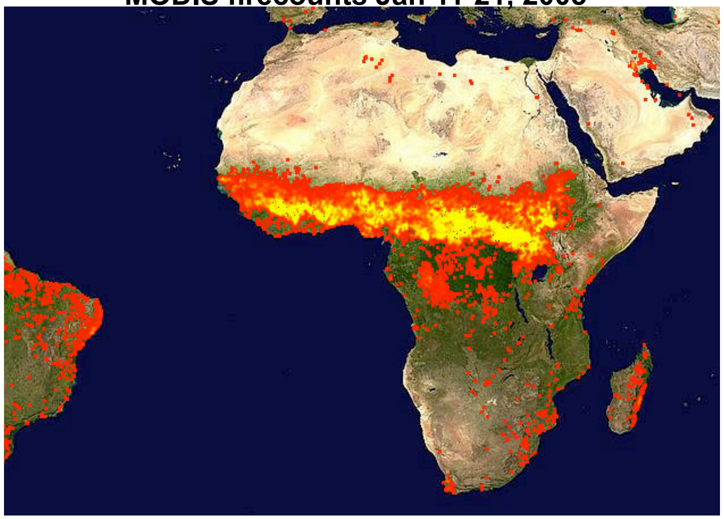

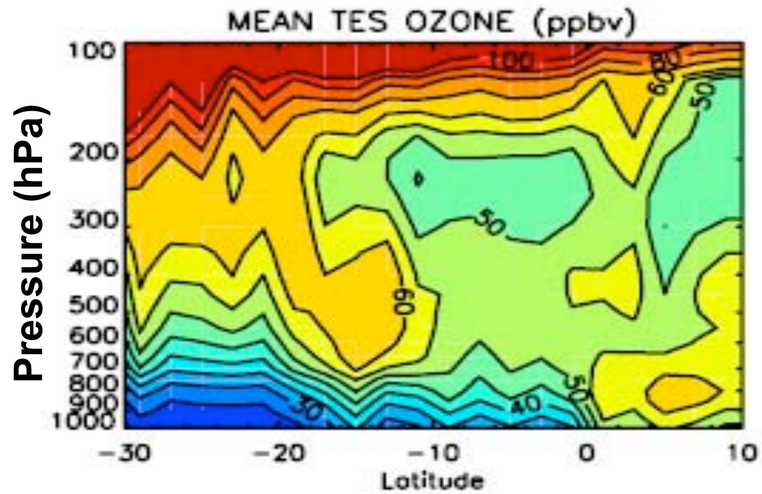

Backward Trajectories from TES

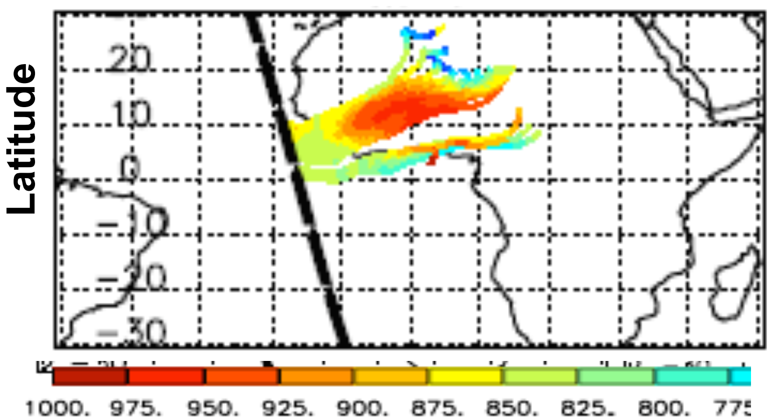

Jourdain (JPL) *et al,* 2007

The tropical Atlantic “paradox” came from TOMS observations of high ozone column South of the ITCZ but low ozone columns North of the ITCZ over Africa during peak biomass burning season (Thompson *et al,* 2000).

With greater sensitivity to the lower troposphere,TES observations show elevated concentrations in the lower troposphere over Africa and in the free troposphere over the tropical Atlantic consistent with in-situ data and model predictions

National Aeronautics and Space Administration
Jet Propulsion Laboratory
California Institute of Technology

Tropospheric Emission Spectrometer

Ozone Production in Boreal Fire Plumes

Case (a) TES O_3/CO 24th July 2006

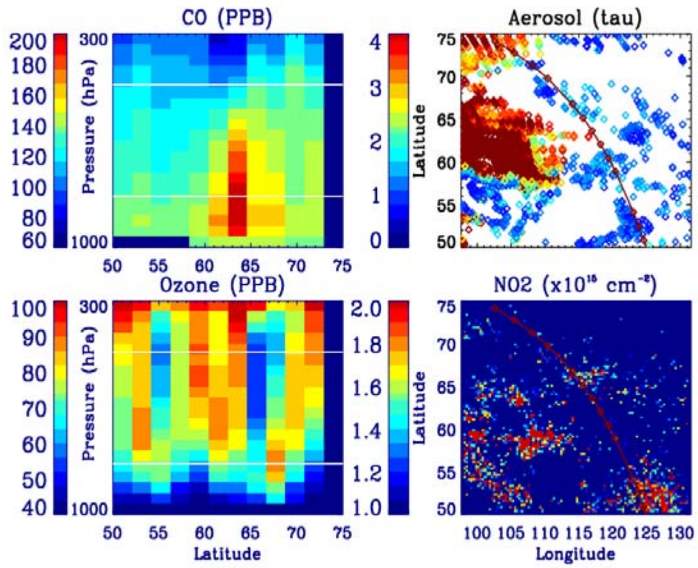

TES OMI

Case (b) TES O_3/CO 24th July 2006

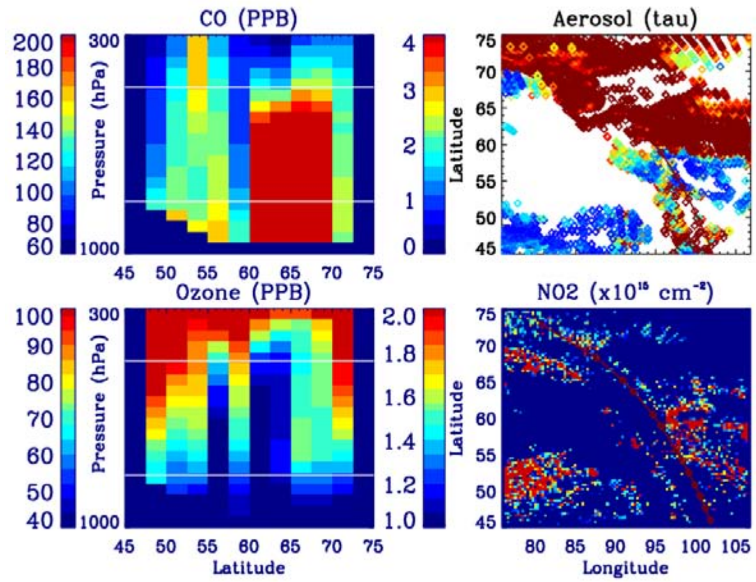

TES OMI

Ozone production in fire plumes is highly variable

- **Based on satellite analysis of observations of CO and ozone from TES in a boreal fire region. Ozone production in these smoke plumes is highly variable. Some plumes show strong ozone enhancement and others show depleted ozone.**
- **Aerosols have a significant impact on the ozone photochemistry.**

(S. Verma et al., 2009)

National Aeronautics and Space Administration
Jet Propulsion Laboratory
California Institute of Technology

Tropospheric Emission Spectrometer

TES used to improve predictions of surface ozone

- Assimilation of TES data into the GEOS-CHEM model greatly improves the agreement between GEOS-CHEM and sonde measurements of tropospheric ozone. In the western US, bias reduced by up to 9 ppb.

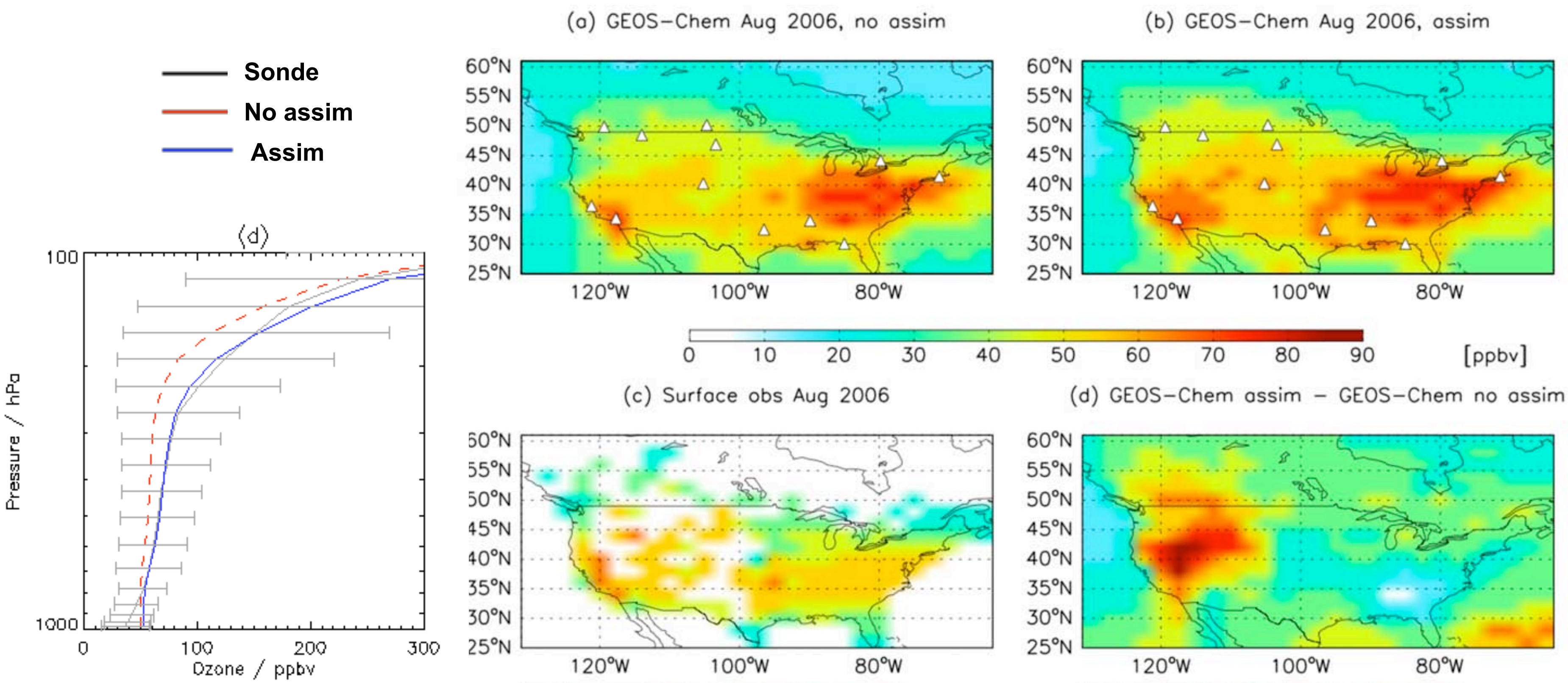

Parrington et al, JGR, 2009

Houston, Texas Air Quality

- Recent experiments were conducted to attribute the air pollution of Houston, TX to sources.
- Regional ozone production preceded 6 of 9 days with high surface values in Houston
- Source Regions for Houston
  - Midwest/Ohio River
  - Chicago
- Regional ozone production preceded 7 of 15 days with high surface values in Dallas
- Source regions for Dallas:
  - Great Lakes/Southern Canada
  - Midwest/Ohio River

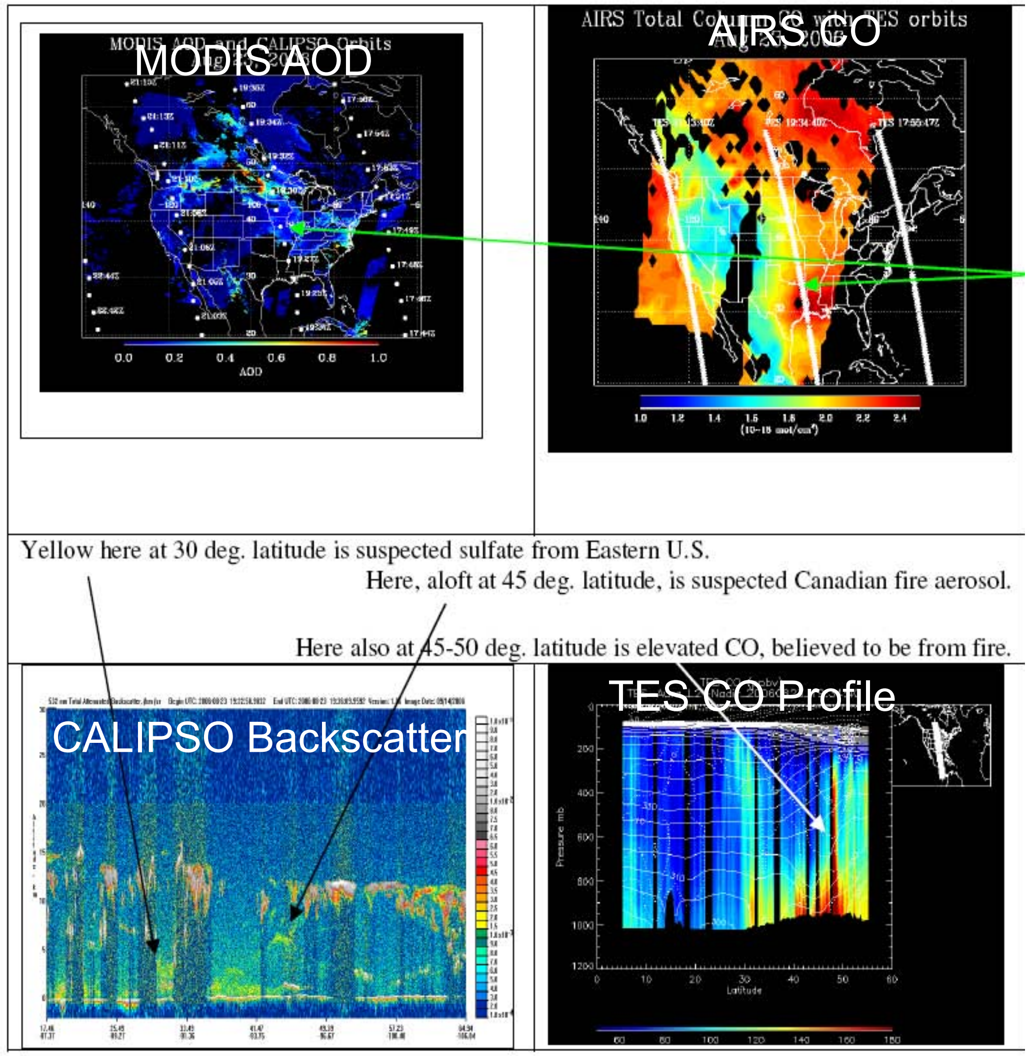

National Aeronautics and Space Administration
Jet Propulsion Laboratory
California Institute of Technology

Tropospheric Emission Spectrometer

Retrievals of Ammonia and Methanol

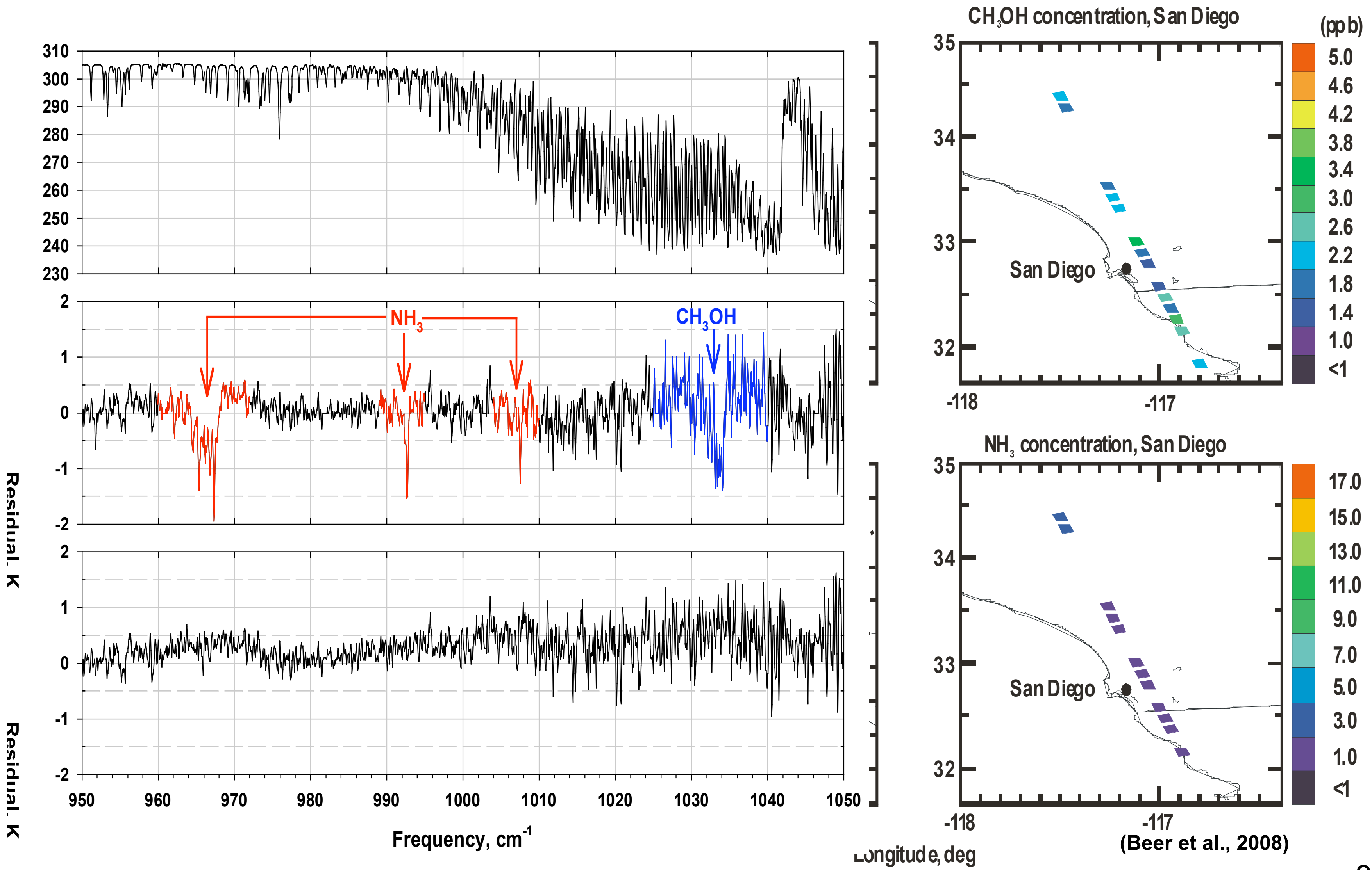

(Beer et al., 2008)

Using and Improving CH_4 Product

TES CH4: representative tropospheric VMR

October 2005 | October 2006 | October 2007

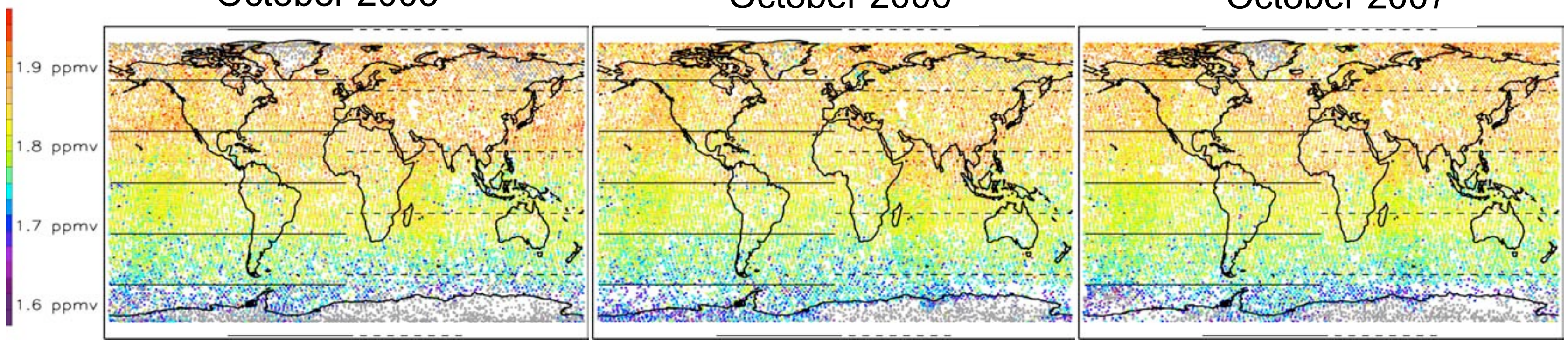

TES RTVMR minus GEOS-Chem 2001 RTVMR field

(after removal of 3.5% high bias from TES and smoothing of difference fields using 2x2 boxcar)

October 2005 | October 2005 | October 2005

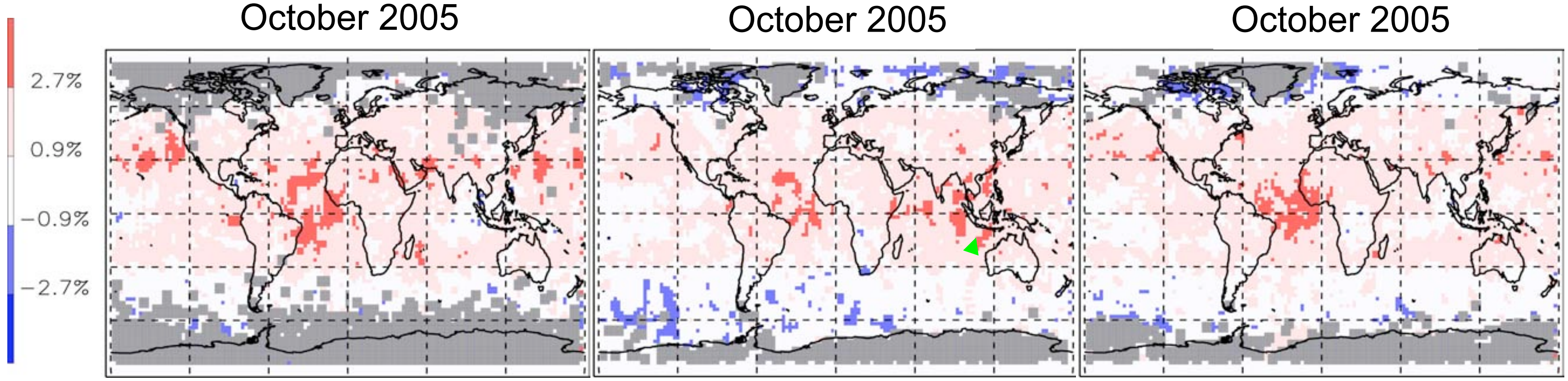

High CH_4 over Indonesia in October 2006 associated with increased biomass burning during the El Nino – collaborating with J. Logan (Harvard) and V. Payne (AER) on interpretation

OMI Tropospheric NO_2 (average Jan.-June 2006)

Gleason, NASA GSFC, Veefkind, KNMI

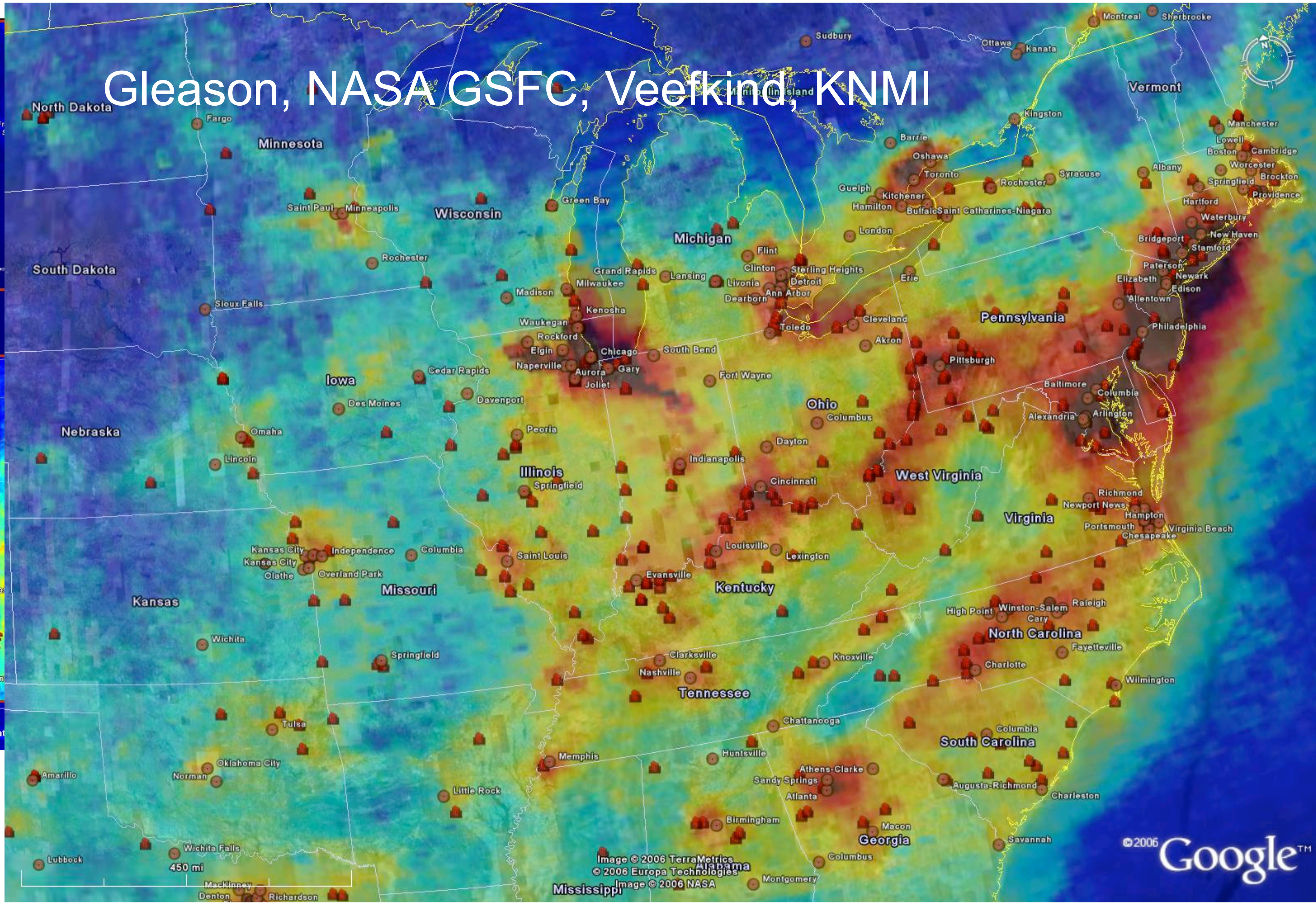

OMI: Monitoring NO_2 emissions in the US

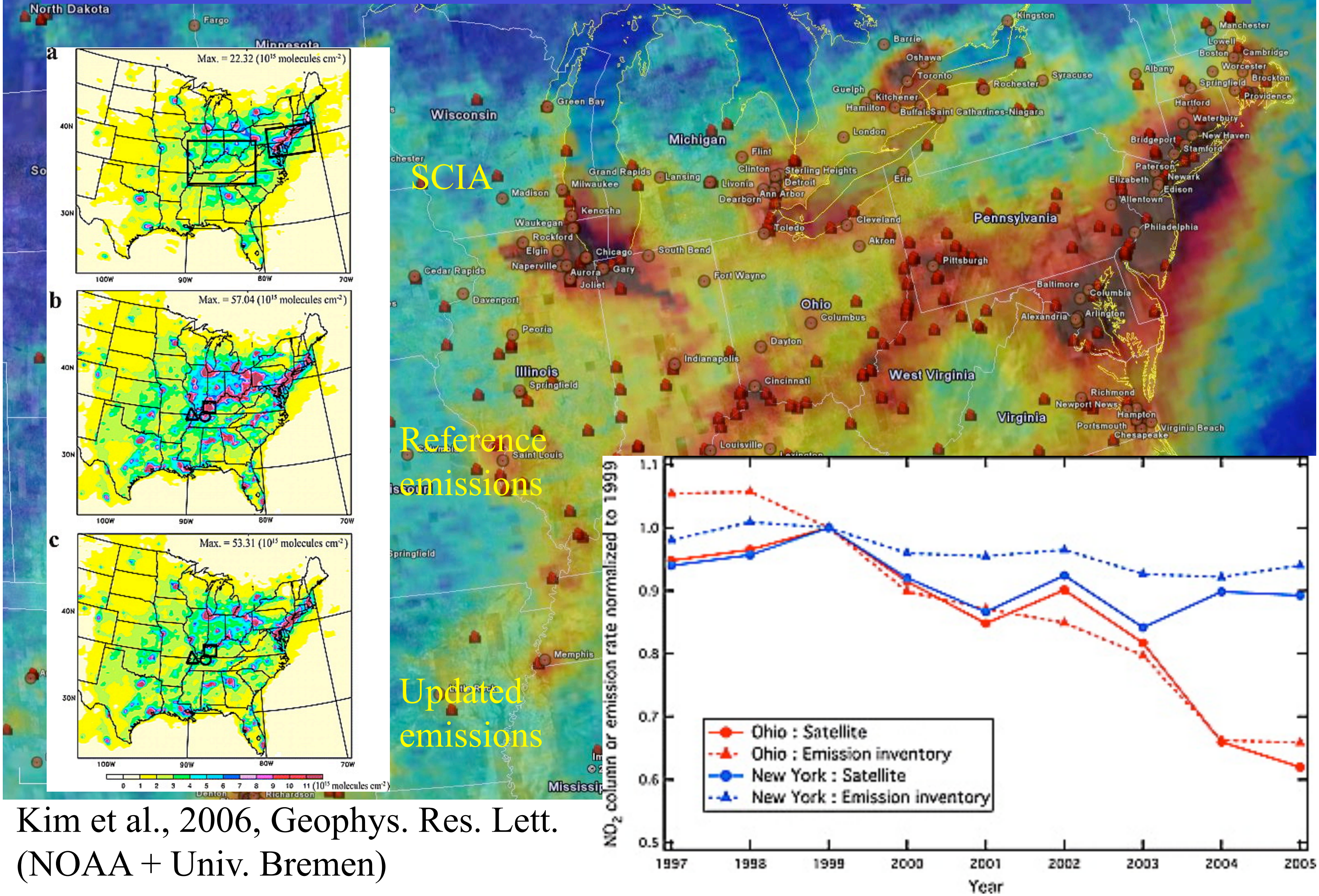

Kim et al., 2006, Geophys. Res. Lett.
(NOAA + Univ. Bremen)

OMI: Sulphur dioxide, SO_2

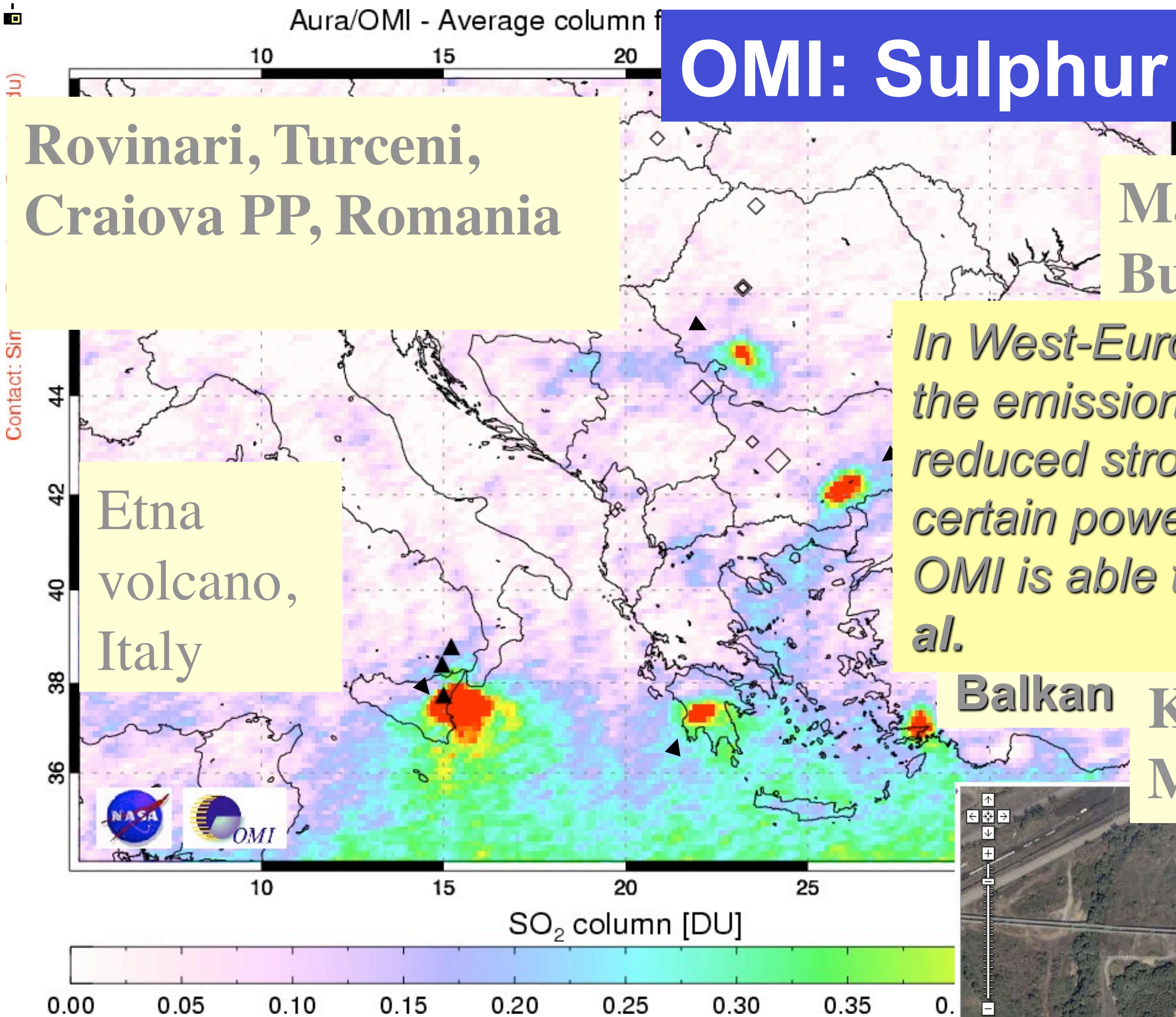

Rovinari, Turceni, Craiova PP, Romania

Maritza Iztok PP, Bulgaria

In West-Europe, the US and Japan the emissions of SO_2 have been reduced strongly. Over China and for certain power plants on the Balkan, OMI is able to detect SO_2. ***Krotkov et al.***

Etna volcano, Italy

Balkan

Kernerkoy complex in Mugla, Turkey

Megalopolis PP in Arkadia, Greece

OMI Average (2005-2006) SO2 burdens over USA, and China

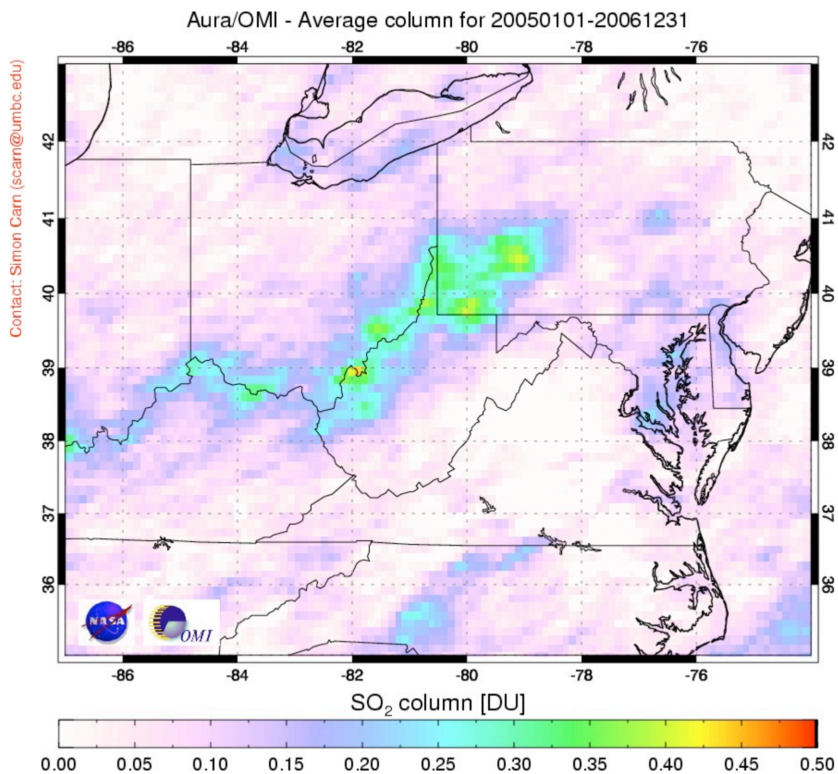

Ohio valley PPs

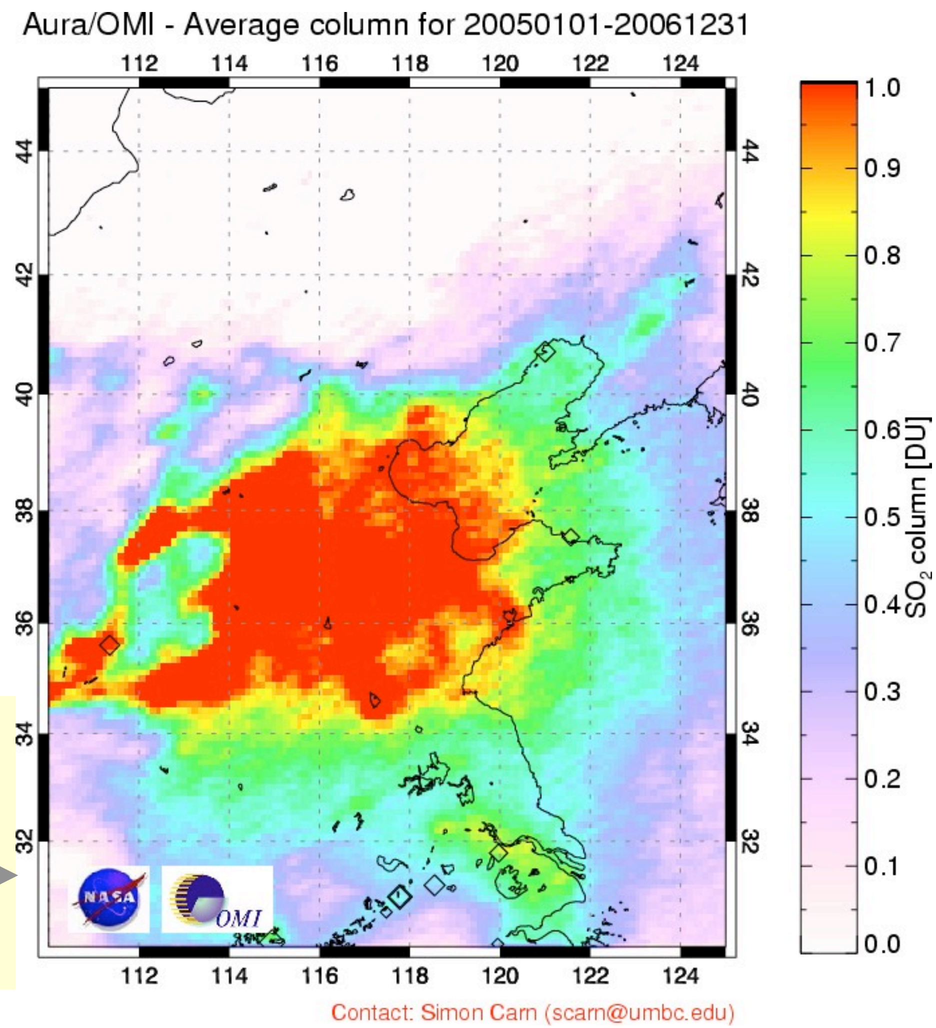

25.5 million tons of SO2 was emitted by Chinese factories in 2005 up 27% from 2000

Krotkov et al.

Comparing emission inventories with OMI measurements

OMI HCHO
Inversed modelling emission Inventory

Millet et al., 2008

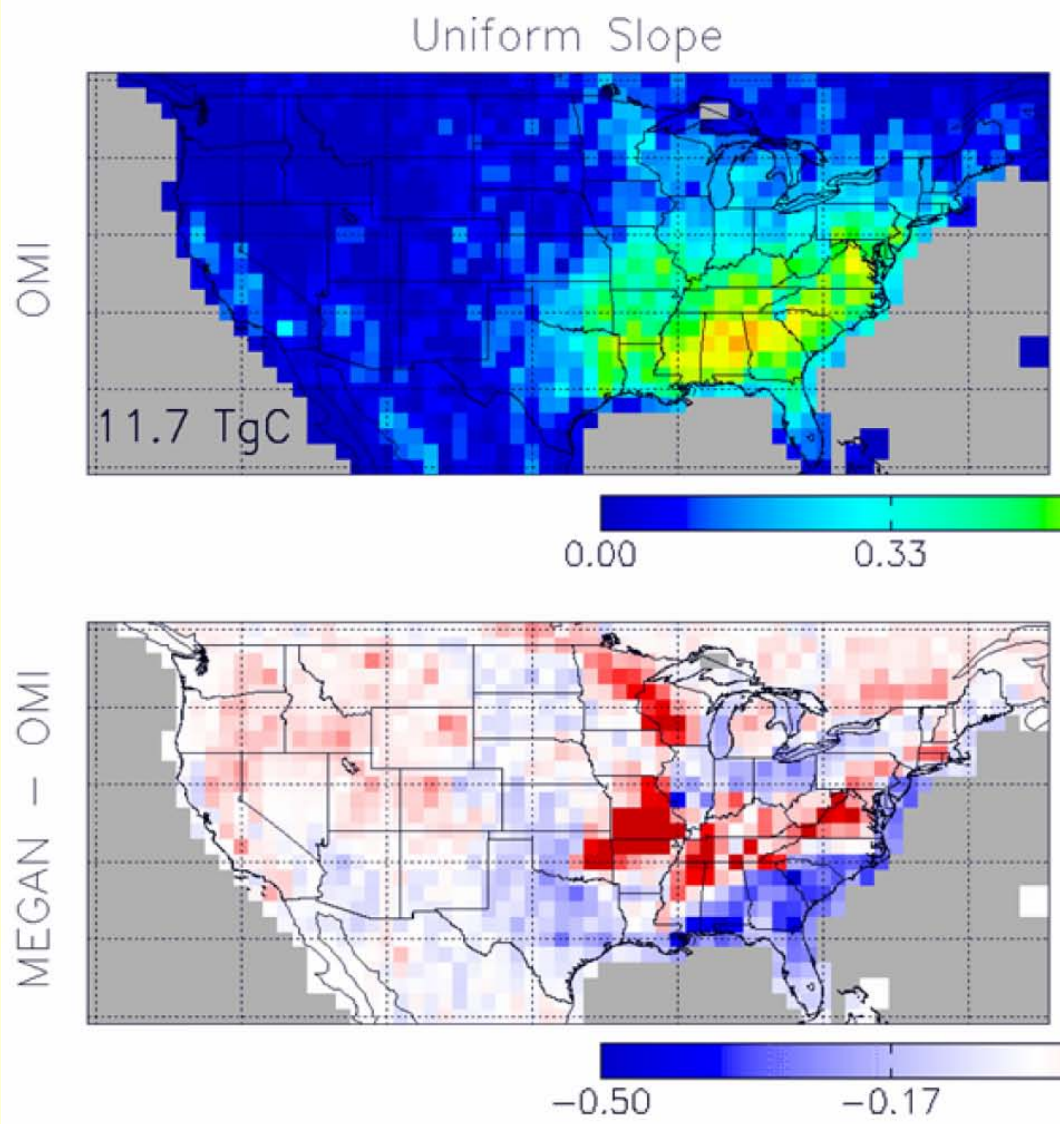

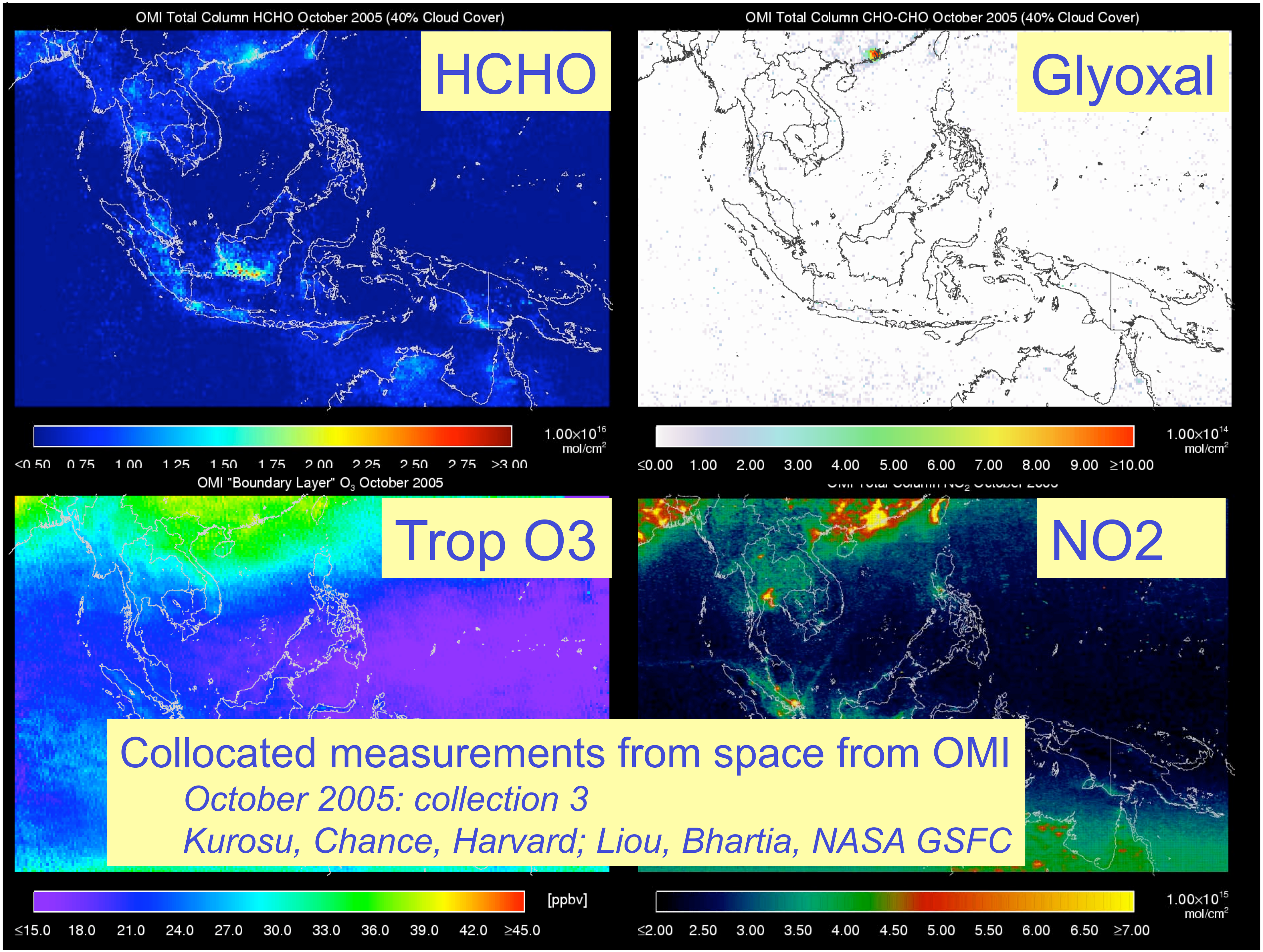

OMI Total Column HCHO October 2005 (40% Cloud Cover)
HCHO
1.00x10^16 mol/cm^2
<0.50 0.75 1.00 1.25 1.50 1.75 2.00 2.25 2.50 2.75 >3.00
OMI Total Column CHO-CHO October 2005 (40% Cloud Cover)
Glyoxal
1.00x10^14 mol/cm^2
≤0.00 1.00 2.00 3.00 4.00 5.00 6.00 7.00 8.00 9.00 ≥10.00
OMI "Boundary Layer" O3 October 2005
Trop O3
[ppbv]
≤15.0 18.0 21.0 24.0 27.0 30.0 33.0 36.0 39.0 42.0 ≥45.0
NO2
1.00x10^15 mol/cm^2
≤2.00 2.50 3.00 3.50 4.00 4.50 5.00 5.50 6.00 6.50 ≥7.00
Collocated measurements from space from OMI
October 2005: collection 3
Kurosu, Chance, Harvard; Liou, Bhartia, NASA GSFC

MOPITT Applications I: Improving African CO Emissions*

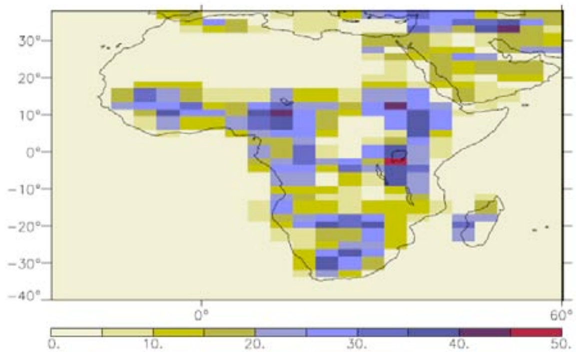

CO Emissions Prior Error

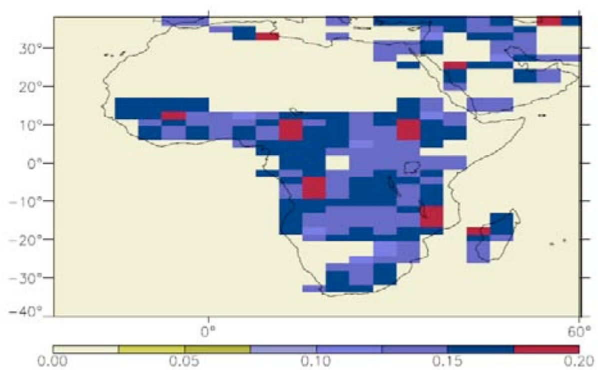

Fractional Emissions Error Reduction (after inversion)

- Inverse modeling using MOPITT data indicates longer burning season, reduced amplitude and interannual variability of seasonal cycle in northern Africa
- Inversion improves fit to independent surface-station measurements by up to 28%

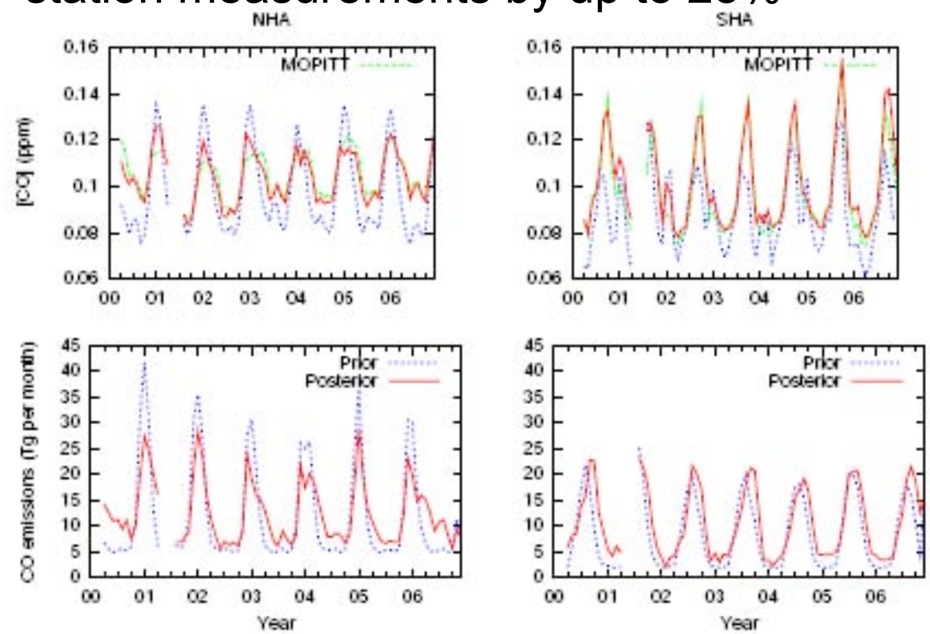

* Chevallier et al., 'African CO emissions between years 2000 and 2006 as estimated from MOPITT observations'. Biogeosciences, vol. 6, January 2009'

MOPITT Applications II: Exploiting Lower-Trop Sensitivity over Indian Subcontinent*

- MOPITT CO sensitivity at surface strongly dependent on 'thermal contrast' between surface and air temperature
- Daytime overpasses of land provide best sensitivity to lower-trop CO

Sensitivity to Surface-level CO

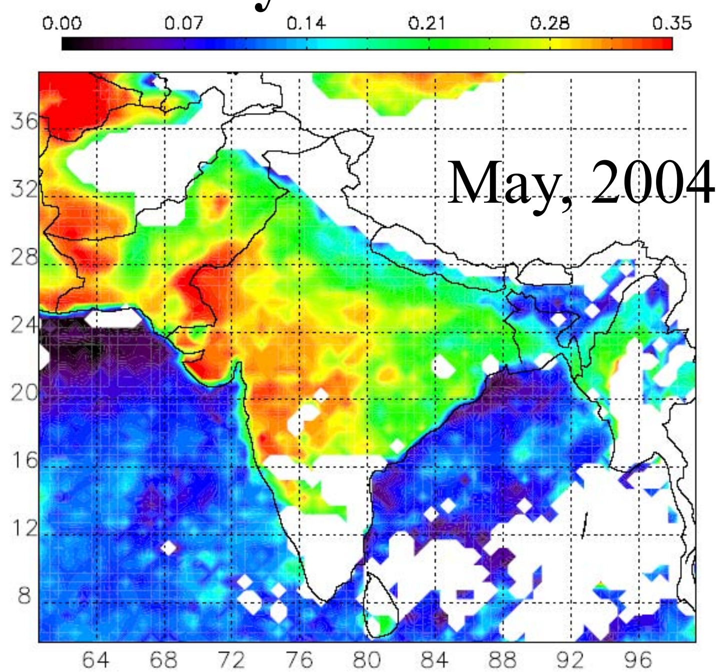

GEOS-CHEM, May 2004

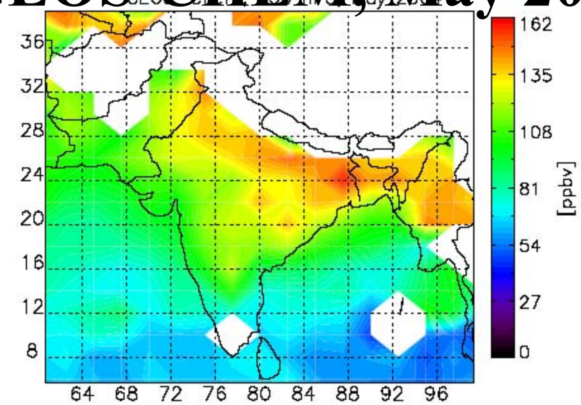

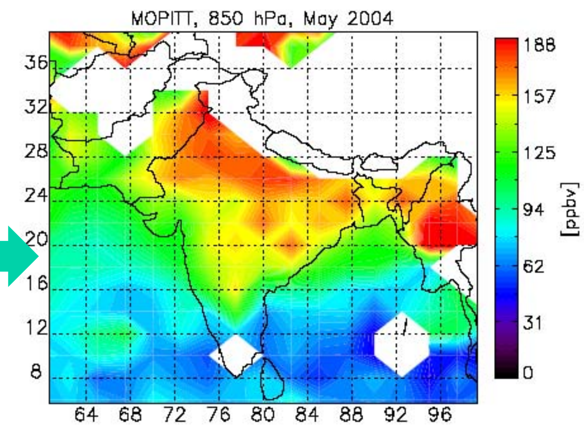

MOPITT 'sees' CO sources in Indo-Gangetic Basin

* Kar et al., 'Measurement of low-altitude CO over the Indian subcontinent by MOPITT,' J. Geophys. Res., 113, 2008

MOPITT Applications III: Exploiting Lower-Trop Sensitivity over China and Megacities*

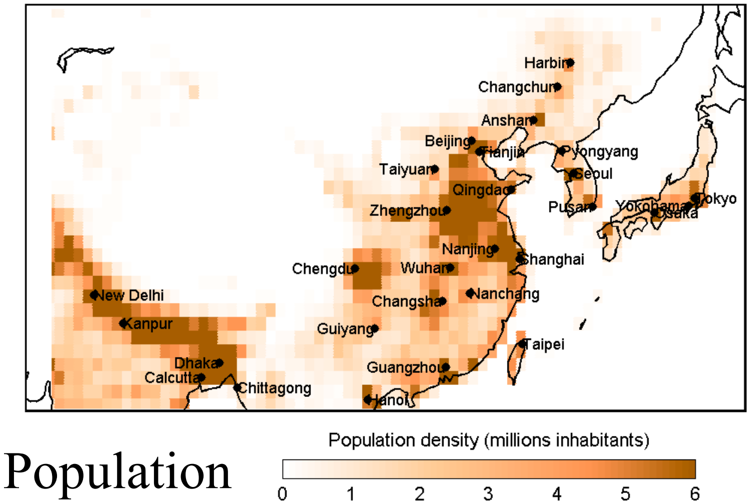

Population

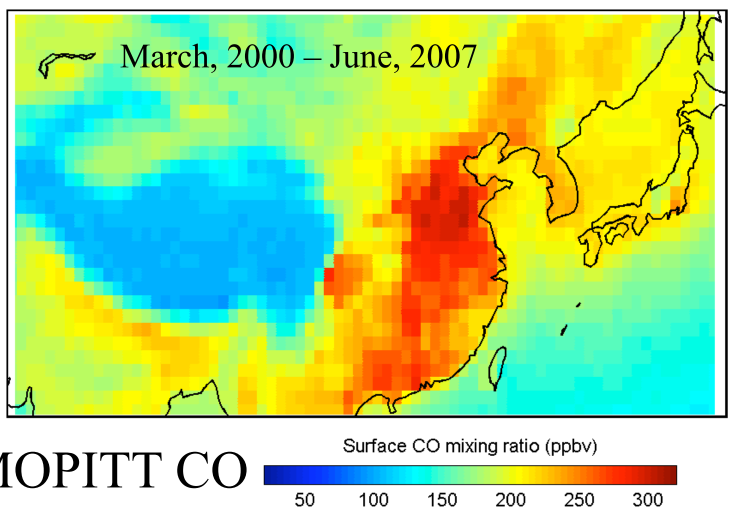

MOPITT CO

- Demonstrated use of MOPITT CO to identify major populations centers, i.e., patterns of urbanization
- Confirmed importance of thermal contrast conditions as determinant of MOPITT's sensitivity to lower-trop CO

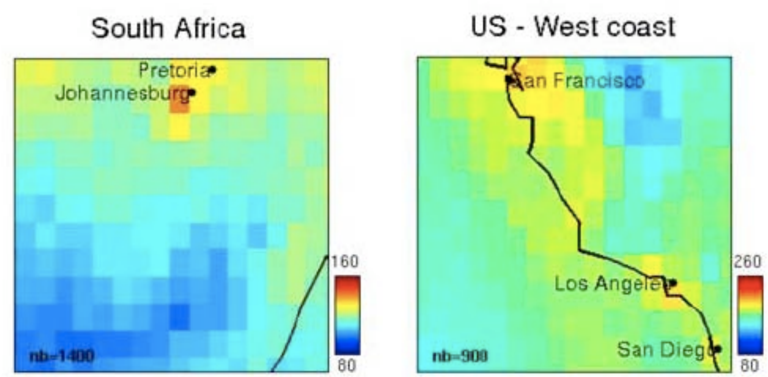

* Clerbaux, et al., 'Carbon monoxide pollution from cities and urban areas observed by the Terra/MOPITT mission,' Geophys. Res. Lett., 35, 2008

Conclusions

- TES, OMI, and MOPITT on the A-train constellation is providing unprecedented vertically resolved chemical observations of the Earth's lower atmosphere.
- Over 5(!) years of measurements data are available.
  - For details and links to data go to:

http://aura.gsfc.nasa.gov

http://terra.gsfc.nasa.gov

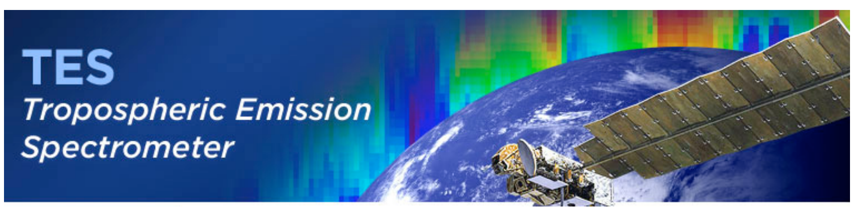

Tropospheric Emission Spectrometer

For more info and links to data centers:

tes.jpl.nasa.gov

Global Views of Ozone and Carbon Monoxide from TES

Lower troposphere (750 hPa, about 2.4 km)

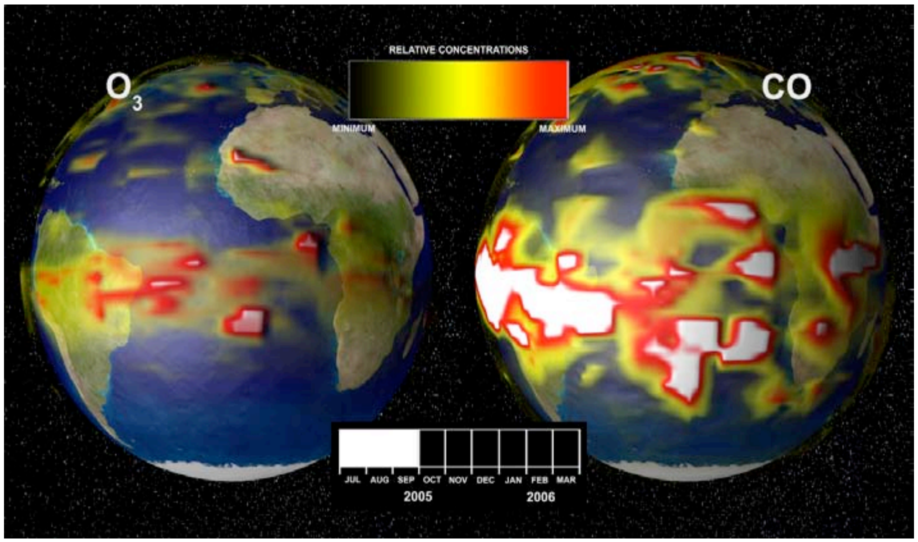

Signatures of southern hemisphere spring biomass burning. September 2005.

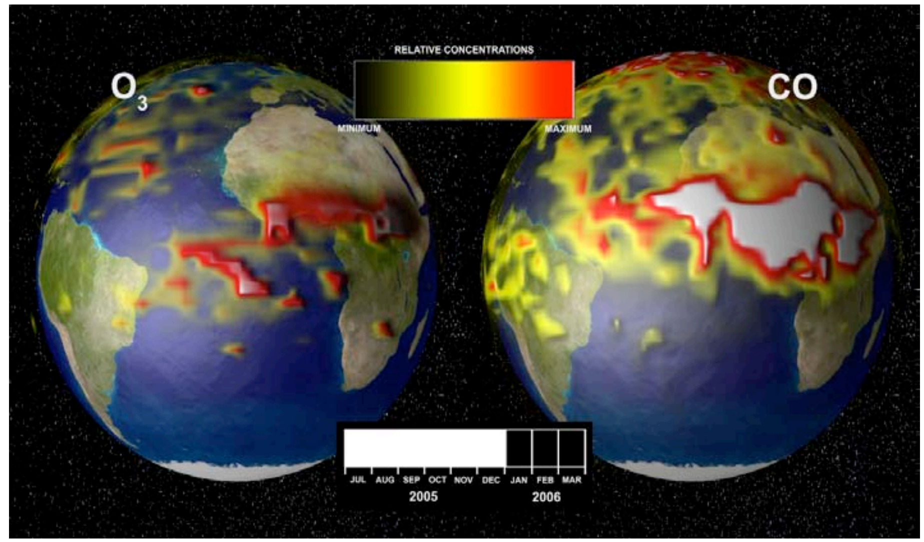

Signatures of Northern Africa winter biomass burning. Dec 2005, Jan 2006.

Tropospheric Emission Spectrometer

National Aeronautics and Space Administration
Jet Propulsion Laboratory
California Institute of Technology

TES Instrument Specifications

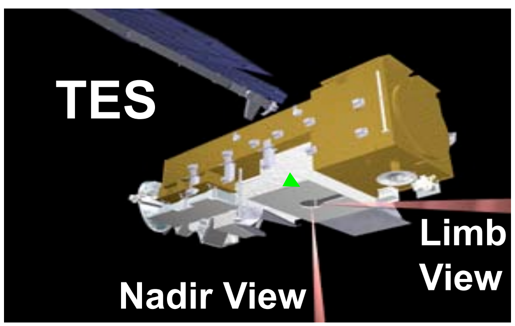

http://tes.jpl.nasa.gov

Spectrometer Type	Connes'-type 4-port Fourier Transform Spectrometer
Max. Optical Path Difference	± 8.45 cm (normal) ± 33.8 cm (hi-res); interchangeable
Scan (integration) Time	4 sec (normal) 16 sec (hi-res)
Sampling Metrology	Nd:YAG laser
Spectral Resolution (unapodized)	0.06 cm^{-1} (normal) 0.015 cm^{-1} (hi-res)
Spectral Coverage	650 to 3050 cm^{-1} (3.2 to 15.4 um)
Detector Arrays	4 (1 x 16) arrays, optically-conjugated, all MCT PV @65K
Field of Regard	45° cone about nadir; trailing limb or cold space; internal calibration sources
Pointing Accuracy	75 urad pitch, 750 urad yaw 1100 urad roll
Max. Stare Time,	208 sec (40 nadir scans)
Spatial Resolution	0.5 x 5 km (nadir) 2.3 x 23 km (limb)
Radiometric Calibration	cavity blackbody (340K) + cold space view
Detector Array Co- alignment	Internal thin slit calibration source
Nadir NESR (Noise Equivalent Spectral Radiance)	2B1 filter: 700 $nW/cm^2/sr/cm^{-1}$ 1B2 filter: 200 2A1 filter: 150 1A1 filter: 100
Nadir NEDT @290K (Noise Equivalent Delta Temperature)	2B1: 1.08 K for 16 detector average 1B2: 0.36 K for 16 detector average 2A1: 0.36 K for 16 detector average 1A1: 2.07 K for 15 detector average